Green Chemistry

COMMUNICATION

View Article Online
View Journal | View Issue

Cite this: *Green Chem.*, 2025, **27**, 14513

Received 12th May 2025,
Accepted 19th October 2025

DOI: 10.1039/d5gc02358k

rsc.li/greenchem

Enhanced production of dimethyl carbonate from the alternating polarity electrolysis of methanol and carbon dioxide

Momoko Ishii,[a,b] Maria M. Paulsen,[a,c] Remi A. Mellinghoff,[a,b] Heather O. LeClerc,[a,b] Ho Yin Tse,[a] Hanno C. Erythropel,[a,b] Julie B. Zimmerman,[a,b] Paul T. Anastas*[a,d] and Darren S. Lee*[a,e]

The alternating polarity methodology in electrochemical synthesis is a procedure where an electrode's polarity is inverted at regular intervals. This technique offers enhanced selectivity, mass transport and can be used to overcome issues with electrode passivation. In this study the application of an alternating polarity protocol to the redox-neutral electrochemical synthesis of dimethyl carbonate (DMC) from gaseous carbon dioxide (CO_2) and methanol was explored using glassy carbon electrodes and catalysed by palladium bromide. Screening different polarity inversion intervals revealed that the DMC yield could be increased up to 482 μmol after 4 h using a 500-second polarity inversion, compared to non-inverting (static) experiments which gave DMC yields of 270 μmol after 4 h. As the reaction proceeded, DMC productivity (as measure of reaction efficiency – *i.e.* how much DMC is being produced per time unit, for instance μmol h^{-1}) was enhanced under the 500 s alternating polarity methodology, nearly doubling after 4 hours compared to the first 30 minutes. On the contrary, productivity was diminished over time in the case of static electrodes. Analysis revealed that under these reaction conditions, methyl formate and formaldehyde were also being formed in competition to DMC. This is attributed to the concurrent oxidation and reduction of methanol and has been confirmed in the absence of CO_2 and Pd. Notably, the presence of CO_2 under alternating polarity led to increased selectivity for DMC.

Green foundation

1. The essence of this work is founded in the Twelve Principles of Green Chemistry in that it is transforming a waste product (carbon dioxide) into a valuable commodity chemical (dimethyl carbonate) through an atom economical transformation using benign reagents and a catalytic process that is employed at ambient temperature and pressure.
2. This study demonstrates a technically simple approach to dimethyl carbonate that combines the use of carbon-based electrodes and an alternating polarity protocol. Together these prevent the deposition of unproductive Pd^0 at the cathode surface and thus, provide a stable reaction that can operate for extended reaction periods (>24 h) without loss in performance.
3. This work supports de-fossilising and detoxifying the chemical industry, a hard to abate sector. But further work is needed to improve electrode efficiencies, reaction selectivity and scalability.

Introduction

The sustainable production of chemicals requires bold new strategies and the utilisation of renewable feedstocks in order to meet net-zero CO_2 emission targets and reduce reliance on finite fossil petrochemical feedstocks.[1] CO_2 is the primary contributor to climate change and it is largely viewed as inert, despite its potential as a valuable chemical carbon feedstock.[2–4] Utilising CO_2 is challenging due to the high energy required to break its carbon–oxygen bonds, however, increasing work on innovative ways to utilise CO_2 as a carbon feedstock is being carried out in the pursuit of a de-fossilised chemical industry, as recently summarised.[5] Recent examples of CO_2 conversion include the synthesis of bulk chemicals, such as methanol,[6] formate,[7,8] and the production of sustainable aviation fuels at tonne scales.[9]

Di-alkyl carbonates (DACs) are another desirable target for CO_2 utilisation, as their use intersects a wide range of indus-

[a]*Center for Green Chemistry & Green Engineering, School of the Environment, Yale University, New Haven, CT, 06511, USA. E-mail: darren.lee@ntu.ac.uk, paul.anastas@yale.edu*
[b]*Department of Chemical and Environmental Engineering, Yale University, New Haven, CT, 06511, USA*
[c]*Department of Energy, Aalborg University, 9220 Aalborg Øst, Denmark*
[d]*School of Public Health, Yale School of Medicine, New Haven, CT, 06511, USA*
[e]*School of Science & Technology, Nottingham Trent University, Clifton Lane, Nottingham, NG11 8NS, UK*

tries and applications, *e.g.* as solvents,[10–12] reagents,[13] fuels[14] and fuel precursors,[15] and for polycarbonate technical materials.[16–18] Amongst this class of compounds, dimethyl carbonate (**DMC**) has gained much attention for its potential as a sustainable building block or as a safer methylating agent compared to metal halides and phosgene.[11,19] While historically, **DMC** synthesis utilised highly toxic phosgene or triphosgene,[20,21] recent attention has turned toward its production from CO_2.[22] One promising methodology involves non-reductive catalysis, where only CO_2, methanol, and a catalyst such as CeO_2 are needed to produce **DMC**, with water as the only by-product.[23] Whilst this thermochemical conversion has been shown to be feasible at scale,[24,25] a major drawback is that this reaction requires the active removal of water to prevent the thermodynamically favoured reverse reaction, *i.e.*, hydration of **DMC** back to CO_2 and alcohol. Thus, the addition of a dehydrating agent into the reaction mixture adds to the stoichiometric waste and/or energy burden upon separation.[26] Our work seeks to address the drawbacks of these previous approaches.

Electrochemistry, ideally utilising renewably-generated electricity, is becoming increasingly popular as a synthetic tool as it offers a greener alternative to traditional thermochemical approaches by providing access to high-energy intermediates and difficult to access scaffolds, whilst circumventing the need for toxic reagents or the stoichiometric generation of waste.[27–30] Given these inherent benefits, electrochemical approaches have been explored for the synthesis of various DACs from CO_2.[31–33] More recently, simple redox neutral approaches have been developed that pair electrochemical CO_2 reduction (CO_2RR) to CO with complimentary oxidation processes, for instance with biomass oxidation,[34,35] or halide oxidation ($2X^-$ to X_2),[36–40] achieving a concerted redox-neutral process (Fig. 1a). Typically, precious metal cathodes, such as Au, Ag, or Pd are required to achieve high faradaic yields for the CO_2RR to CO step and thus high yields of DACs.[41–43] Table 1 outlines the key developments in the merging of redox neutral electrochemical CO_2RR to CO with Pd carbonylation catalysis. Since the initial report with Au, there have been several efforts to develop more efficient electrode materials that allow for a higher faradaic efficiency (FE) to CO.

Alternating polarity is a protocol in electrochemical synthesis whereby the electrodes flip polarity at a given frequency ranging from milliseconds to minutes (Fig. 1b). This electrochemical approach has recently been demonstrated to boost reaction performance, overcome mass transport limitations, and prevent electrode passivation in a range of different electrochemical transformations.[44–47] In some cases, this approach even yielded previously unfavoured products. To date, the implementation of alternating polarity methodologies applied to CO_2RR have been mostly limited to pulsed potential methodologies, where the cell potential is alternated between different potentials rather than inverted negative to positive.[48–50] Herein, we report the synthesis of dimethyl carbonate (**DMC**) from CO_2 and methanol with a Pd catalyst harnessing negative/positive alternating polarity to boost the reaction productivity, reaction selectivity and faradaic efficiency.

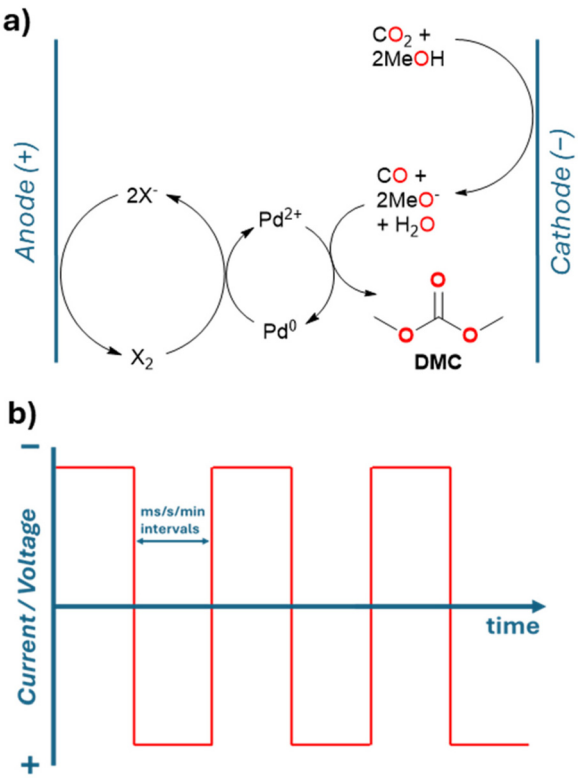

Fig. 1 (a) Reaction scheme showing the redox-neutral approach to dimethyl carbonate (**DMC**) from methanol and carbon dioxide catalysed by palladium and a halide. (b) Simplified graphical representation of an alternating polarity waveform, where the polarity of the working electrode switches at a set time interval or frequency, which can be in the range of milliseconds to minutes.

Results and discussion

Exploring optimal electrode materials

Our initial experimental work focused on identifying suitable readily available electrode materials that could be applied in an alternating polarity set-up whilst remaining amenable to a scalable flow reactor. Whilst gold cathodes provided the highest faradaic efficiency for the CO_2RR to CO step (Fig. 2a), they were deemed unsuitable for alternating polarity due to the potential for degradation and leaching of AuX_3 salts when run as the anode in the presence of halide based supporting electrolytes.[51] Indeed, the utilisation of a gold-plated electrode as the anode coupled with a $PdBr_2$ catalyst resulted in significant electrode degradation (Fig. 2b) and ICP-MS revealed dissolved Au in solution (>7300 ppb, Table S1). In addition, significant degradation of the electrode surface was confirmed by SEM-EDS (Fig. S3) and XPS (Table S2).

Switching the anode to carbon-based electrodes (*i.e.*, graphite or glassy carbon) avoided metal leaching and provided a stable anode to facilitate the $2X^-$ to X_2 oxidation process (Fig. 1a). Using a graphite anode, we then screened a range of cathode materials and found the reaction proceeded with all cathode materials evaluated (Fig. 2a), albeit, as expected, with

Table 1 Showing a comparison of the key developments in redox-neutral formation of dimethyl carbonate from CO_2 and methanol. FE = faradaic efficiency, J = current density. Productivity was calculated using J and FE, see ESI for detailed calculations

Ref.	Cathode	FE (**DMC**)	Productivity (μmol cm^{-2} h^{-1})	Catalyst	J (mA cm^{-2})
36	Au	55–60%	134	40 mg 20% Pd on C	12
31	Ni single atom	80%	179	40 mg 10% Pd on C	12
38	B-doped Pd	47.5% (1 h) 35.6% (3 h)	266	Pd-B on cathode	30
39	Co-CPY/CNT	—	96 (0.2 MPa)	40 mg Pd/C	16

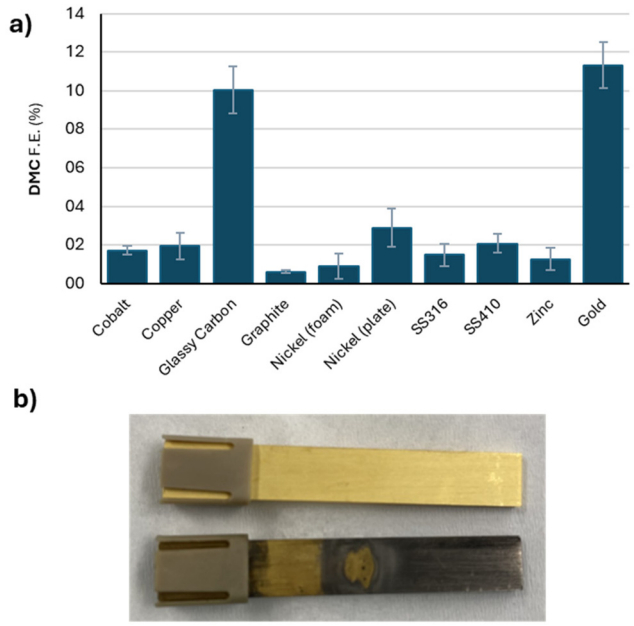

Fig. 2 (a) Faradaic efficiency comparison of cathode materials for dimethyl carbonate (**DMC**) production – run under standard batch conditions at 5 V. F.E. = faradaic efficiency, SS = stainless steel. Error bars representing ± one standard deviation. (b) An example of degradation observed when using gold electrodes before (top) and after (bottom) a 4 h static experiment.

reduced faradaic efficiency (FE) for **DMC** compared to gold. Surprisingly, glassy carbon (GC) as the cathode resulted in similar **DMC** FEs compared to gold (10.0% *versus* 11.3%, Fig. 2a). Given this similarity in performance and its inherent stability, we chose to pursue this material in the alternating polarity methodology.

Alternating polarity optimisation

Using glassy carbon as both anode and cathode, we next explored different intervals for the alternating polarity protocol. Experiments were conducted in constant voltage mode, as preliminary investigations showed that in constant current mode, reactions would often fail to maintain the necessary potential to continuously produce **DMC** and led to variable results (not shown). Next, several fixed voltages were screened with a 4 h reaction time, which was chosen in order to allow a significant amount of **DMC** to form for accurate analysis: At 2 V and 3 V, negligible **DMC** was formed while at 6 V the yield obtained was higher than at 5 V (731 *versus* 477 μmol, respectively; Fig. S11). However, at 6 V we observed frequent fluctuations in the current, which was at, or close to, the 100 mA upper current limit of the utilised ElectraSyn™ unit, and also a significant drop in the selectivity to **DMC**, which is discussed in detail later (see Fig. 6a). We therefore chose 5 V due to the combination of the highest yield of **DMC** whilst maintaining a stable current (see Fig. S11). Next, a range of polarity alternation frequencies were tested using the 5 V constant voltage condition and a reaction time of 4 h, where CO_2 was continuously bubbled through methanol at a rate of 1 mL min^{-1} (Fig. 3a). In this setup, lithium bromide served as both the supporting electrolyte and as a source of bromide for the anodic counter oxidation reaction, and $PdBr_2$ as the carbonylation catalyst. Most alternation intervals outperformed the static polarity setups (Fig. 3b and see also Fig. S8), with the exception of the 50 ms condition. The highest yield was observed at a 500 s interval (482 μmol **DMC**), nearly doubling the yield of the static polarity setup (270 μmol **DMC**).

Sampling across the 4 h reaction experiment using GC electrodes revealed increasing productivities (in μmol h^{-1}) with time for the 500 ms, 500 s, 1800 s, and 3600 s polarity switching conditions (Fig. 3b) while the static conditions did not exhibit this trend of increasing productivity. Under the static conditions a decrease in productivity over the same timeframe for both GC and gold electrodes was observed (Fig. 3c and Fig. S8). Further experiments using GC electrodes with the polarity switching every 500 s over a 12 h timeframe demonstrated that productivity initially increased but remained relatively constant around 113–115 μmol h^{-1} after the 2 h mark (Fig. 3c). In contrast, when performing the same experiment using GC electrodes but without polarity switching, productivity was 4–5 × lower (<27 μmol h^{-1}) than with polarity switching over the 12 h period (Fig. 3c). Finally, the overall yield at 12 h reaction time of 1368 μmol tracked closely with the observed combined productivity for the experiment (Fig. 3d).

During the static polarity reactions, we observed a colour change in solution from orange-brown to yellow as well as black material build-up on the surface of the GC cathode (Fig. 4a, left), which we postulated to be Pd^0 (E° = 0.915 V).[52] This hypothesis was reinforced by an observed large decrease in Pd^{2+} concentration in solution measured by ICP-MS (Fig. 4b). Conversely, when we applied the alternating polarity approach at an interval of 500 s using GC electrodes, we observed that the reaction mixture maintained the same

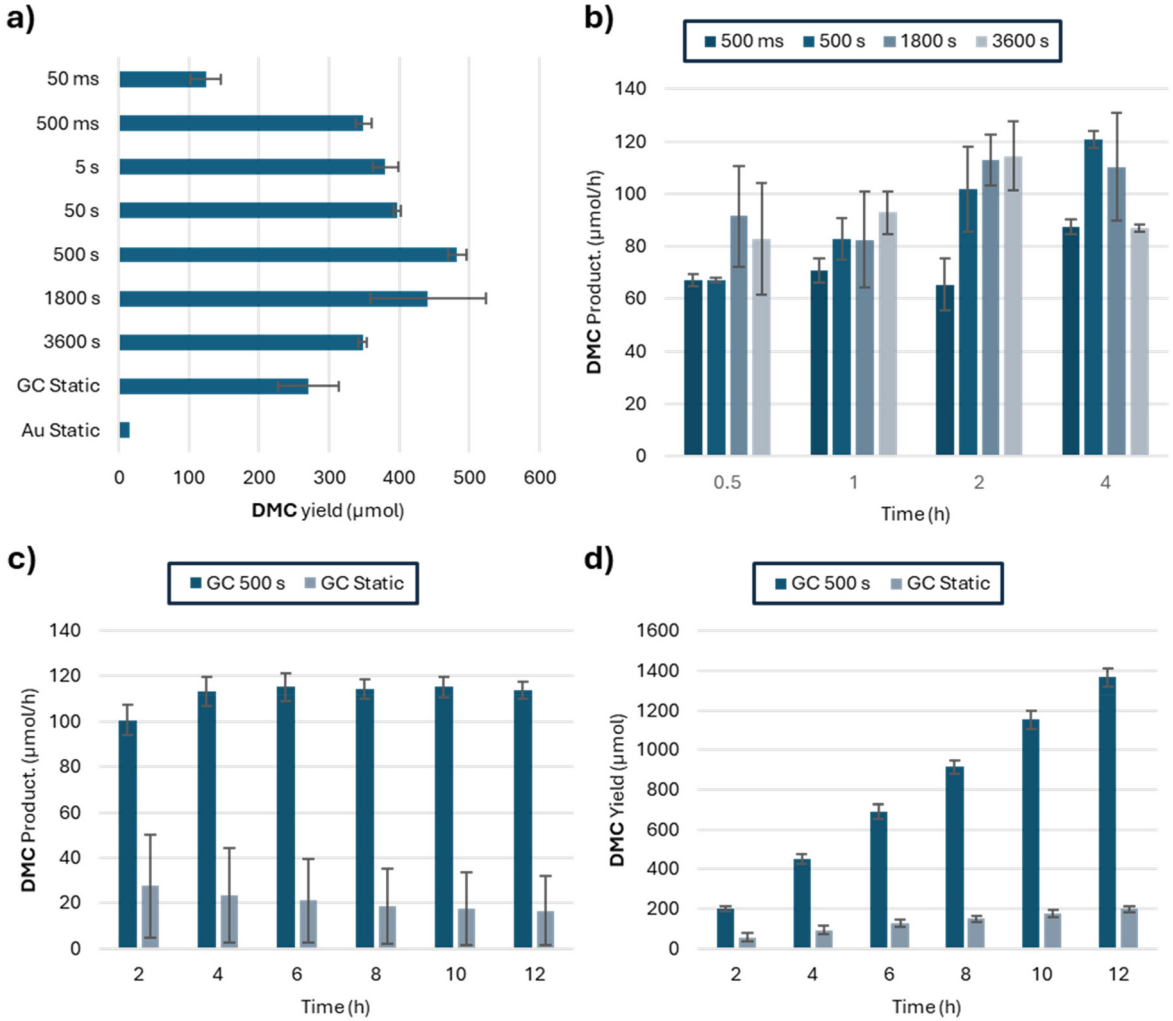

Fig. 3 (a) **DMC** yields at 4 h for different polarity alternation intervals using glassy carbon (GC) electrodes, and two static conditions for GC and gold (Au); time-resolved **DMC** productivity in μmol h^{-1} at select frequencies of alternating polarity and 5 V using GC electrodes (b) over 4 h; and (c) over 12 h with a comparison to the static condition (no alternation); (d) time-resolved **DMC** yield in μmol using alternating polarity (500 s) or static conditions at 5 V. Error bars representing ± one standard deviation.

orange-brown colour throughout the experiment with no significant build-up on the electrodes (Fig. 4a, right). In addition, ICP-MS confirmed that the Pd^{2+} concentration in solution remained stable, suggesting negligible metal deposition occurs (Fig. 4b). At intervals >500 s, we did visually observe temporary Pd^0 build-up on the cathode, however, following polarity switching, this build-up would gradually disappear from the electrode surface, suggesting dissolution of metallic Pd^0. Based upon these observations, a potential rationale for the increase in productivity with alternating polarity could be attributed to the relatively higher concentration of Pd^{2+} in solution compared to the static mode, where Pd^{2+} deposits as Pd^0 on the electrode, thereby effectively removing it from the solution and stalling the catalytic carbonylation step, thus leading to a decrease in **DMC** productivity. These results suggest that alternating the polarity allows for a more stable concentration of available Pd^{2+} in solution, thus enabling the catalytic carbonylation step to proceed steadily and therefore maintaining a consistent level of formation of **DMC** from the components of the CO_2RR (Fig. 4c). In addition, SEM-EDS comparing the GC electrode surface prior to the experiment (Fig. S4) with both GC electrodes following a 4 h experiment under a 500 s polarity switching regime (Fig. S5 and S6) showed only minimal deposited Pd^0 on the surface (and some Br), which further confirms that Pd^{2+} is not built up in excess on the electrode surface and instead remains predominantly in solution under these conditions. In contrast, an SEM-EDS of the GC cathode after 4 h in static conditions showed a visible deposited layer over the GC electrode surface as well as significant amounts of Pd (Fig. S7). Whilst some reports have described Pd containing electrodes capable of facilitating a higher level of CO_2RR to CO, we have little evidence that this is the case in our system.[38] Cyclic voltammetry using glassy carbon electrodes and a Ag/AgCl reference electrode performed on a solution containing $PdBr_2$ (0.5 mg mL^{-1}) with LiBr (0.1 M) in methanol revealed an enhancement in the redox activity

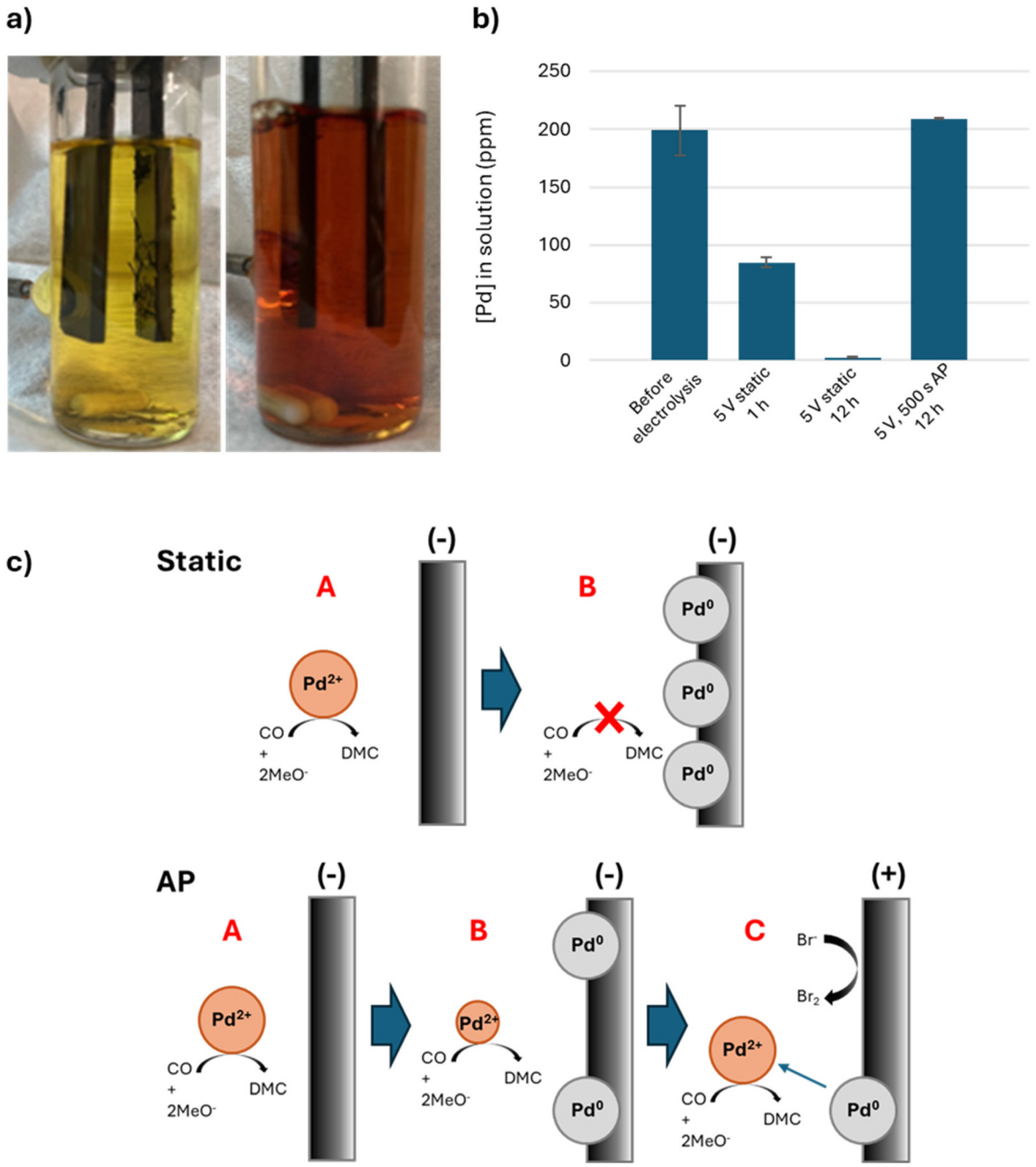

Fig. 4 – (a) Photo of reaction mixture and GC electrodes after experiments for 4 h at 5 V, left: using static conditions, right: using polarity switching every 500 s. (b) Showing the concentration of Pd species (measured by ICP-MS, also see ESI) in solution before electrolysis occurs, under static polarity conditions (5 V, 1 h and 12 h) and under alternating polarity conditions (5 V, 500 s, 12 h) (c) Scheme of the proposed effect of alternating polarity: *Under static conditions (top)*: (A) At the beginning of the reaction the Pd^{2+} concentration in solution is high so **DMC** formation can occur. As electrolysis begins Pd accumulates at the cathode through electrostatic interaction. (B) Pd^0 deposition occurs on the cathode; Pd^{2+} concentration in solution decreases therefore **DMC** production is reduced. *Under alternating polarity (AP) conditions (bottom)*: (A) At the beginning of the reaction the Pd^{2+} concentration in solution is high so **DMC** formation can occur. As electrolysis begins Pd accumulates at the cathode through electrostatic interaction. (B) Pd^0 deposition begins to occur on the cathode. (C) The polarity inverts and the cathode that has accumulated Pd^0 is now the anode. Bromide oxidation now begins to occur on this "new" anode in the presence of Pd and facilitates the efficient re-oxidation of Pd^0 to Pd^{2+}, subsequent dissolution occurs, and **DMC** formation increases. Pd^0 deposition begins again on the "new" cathode. The polarity then inverts again, and the cycle continues until the system reaches a steady-state.

of the Pd species in the presence of CO_2 compared to an N_2 saturated solution (Fig. S21), suggesting there is an increase in the Pd^{2+}/Pd^0 activity possibly from the formation and consumption of CO, however further investigation is needed to probe the possibility of Pd enhancement of CO_2RR at the electrode surface. Based on our evidence, we hypothesise that the

enhancement in reaction efficiency by switching the polarity regions predominantly comes from the increase in mass transport and the increase in the rate of oxidation of Pd^0 to Pd^{2+}.

Reaction selectivity

To determine the selectivity of the reaction using polarity switching at 500 s, an investigation of the reaction mixture by gas chromatography with flame ionisation detection (GC-FID) revealed that methyl formate (**MF**) and formaldehyde (**FA**) were being formed concurrently with **DMC**. We postulated that **FA** is likely to result from the competing anodic oxidation of methanol (Fig. 5b).[53] **MF** could result from a competing CO_2RR process to yield formic acid with subsequent esterification with methanol to **MF** (Fig. 5c). However, in the absence of CO_2 we still observed **MF** formation, suggesting the primary source was a redox-neutral process whereby methanol oxidation and reduction occur simultaneously. Methoxide in the presence of Br_2 from the anodic oxidation of LiBr can then form MeOBr, which in turn can undergo addition to **FA** to yield **MF** (Fig. 5b).[54]

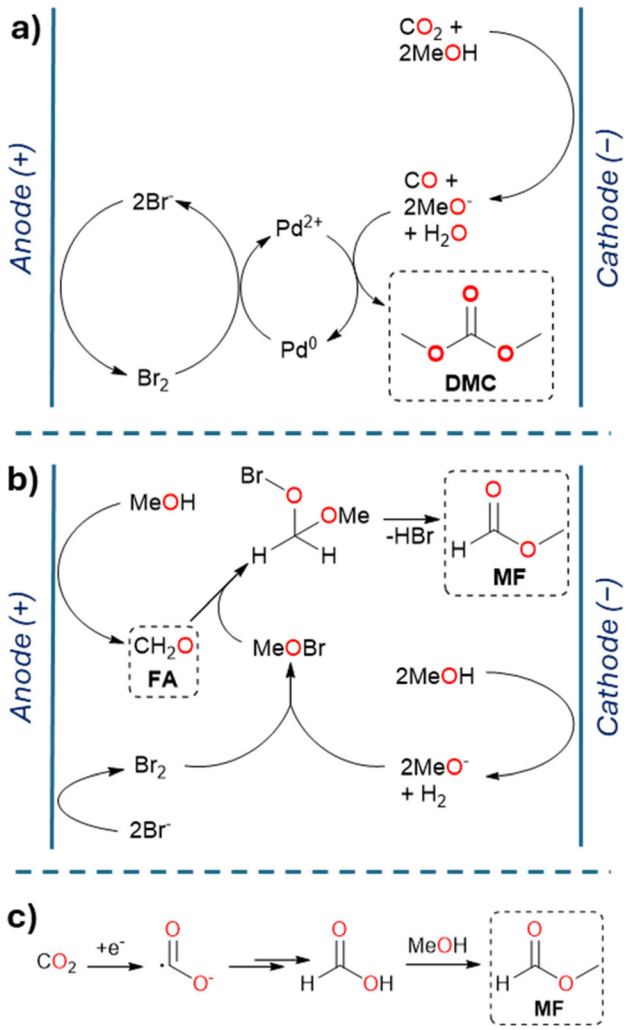

Fig. 5 Demonstrating the competing reaction pathways potentially occurring in the electrochemical cell. (a) The redox-neutral formation of **DMC** in the presence of MeOH, CO_2 and LiBr. (b) Showing the redox-neutral formation of **MF** from MeOH and LiBr. (c) Possible formation of **MF** from CO_2 *via* reduction of CO_2 to formate and then subsequent formation of formic acid and esterification with methanol.

We postulated that the onset of these reactions might occur at different voltages and hence have different selectivity at different applied potentials. Tracking each of these compounds in an experiment using alternating polarity at 500 s, we observed that **MF** was formed as the primary product at 2 and 3 V (Fig. 6a). At 4 V and 5 V, the amount of **DMC** produced in the reaction was comparable to **MF**, and at 6 V we found reduced selectivity toward **DMC** despite an increase in yield, which we speculate is due to increased hydrogen gas production from an increase in methanol reduction (as observed with an increase in **MF** yield) causing the availability of dissolved CO_2 to fall.[55]

Interestingly, despite the yield of both **DMC** and **MF** increasing over the 4 h reaction time (Fig. 6b), the productivity of **MF** fell where the productivity of **DMC** increased (Fig. 6c). Reducing the electrode surface area to approx. 42% of the original gave comparable results, suggesting that the reaction is not limited by electrode surface area or mass transfer at the electrode surface (Fig. 6d). Further control experiments revealed negligible production of the three products when no electricity was applied to the cell (Fig. S13), whilst in the absence of Pd, small amounts of **DMC** were observed when a current was applied (Fig. 6d). Interestingly, in the absence of Pd and CO_2, **MF** was still produced in quantifiable amounts; however, introducing CO_2 in the absence of Pd led to a significant fall in the **MF** yield obtained (3352 and 488 μmol, respectively; Fig. 5d right *Y*-axis). This decrease in the **MF** yield in the presence of CO_2 aligns with the observation of Lee *et al.* that MeOBr production is inhibited in the presence of CO_2.[36] With Pd present in the reaction mixture, significant amounts of **DMC** and **MF** were observed both when the reaction was run under air or under an N_2 atmosphere (Fig. 6d). Whilst the **DMC** yield was not as high as in the presence of both Pd and CO_2 (134 *vs.* 478 μmol; Fig. 6d), it is clear that a secondary mechanism is operating in tandem with the CO_2RR and producing **DMC** from MeOH, **MF** or **FA** or a combination of these components without the need for CO_2. To confirm the necessity of bromide in the reaction mixture, control reactions were performed under the optimal conditions, replacing $PdBr_2$ with $Pd(OAc)_2$ (Fig. S14). Changing the Pd source gave negligible difference in both the yields of **DMC** and **MF**, however removing bromide from the system all together led to a more profound change in the **DMC** yield. When the LiBr supporting electrolyte was exchanged for a non-halide salt, *i.e.* tetrabutylammonium tetrafluoroborate (NEt_4BF_4), we found that **DMC** was undetectable by GC-FID, whilst **MF** production continued at a similar level to normal (Fig. S15). Interestingly, this result does imply that bromide is necessary for the formation of **DMC**, but its absence does not seem to impact the formation of **MF**. Overall, the production of **MF** is comparable to that of **DMC** in our system and reducing the amount formed requires careful attention.

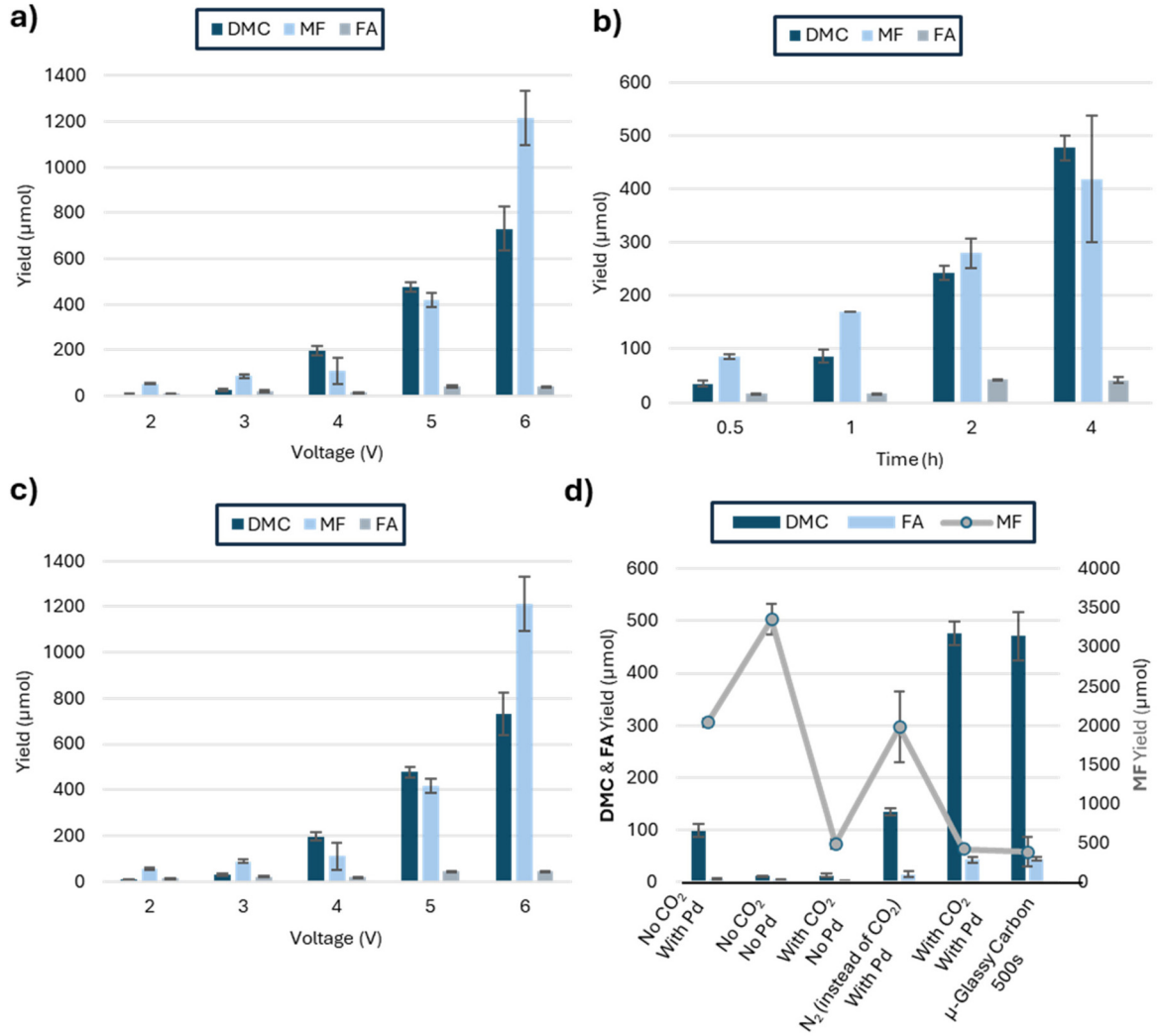

Fig. 6 Yield of dimethyl carbonate (**DMC**), formaldehyde (**FA**), and methyl formate (**MF**) after a reaction using 500 s alternating polarity (a) at various voltages after 4 h and (b) sampled at various times using 5 V; (c) productivity of **DMC**, **FA**, and **MF** under same conditions as in (b); (d) yield of **DMC**, **FA** and **MF** under different control conditions using, unless otherwise indicated, 5 V and 500 s polarity switching and a 4 h reaction time. Surface area of the μGC electrodes reduced by approx. 58% assuming no porosity (regular GC: 52.5 mm × 8 mm × 2 mm *vs.* μGC: 56 mm × 3 mm × 1 mm). Error bars representing ± one standard deviation.

Conclusion

The application of alternating polarity protocols to the redox-neutral electrochemical production of dimethyl carbonate (**DMC**) has been reported. Whilst the faradaic efficiency of this system is lower than some literature reports, the productivities and yields are in a similar range. In addition, we have demonstrated the importance of maintaining the active Pd^{2+} species for the effective formation of **DMC** and how alternating the polarity can greatly enhance this process in order to deliver a stable reaction over extended periods of time. Alternating the polarity greatly enhanced reaction stability and reduced the build-up of palladium on the electrode surface. The polarity alternation interval of 500 s was found to be optimal resulting in both the highest yield and productivity for **DMC** in this electrocatalytic system. In the case of gold and glassy carbon electrodes under static conditions, Pd deposition likely limited the reaction utility by removing the active species Pd^{2+} necessary for **DMC** production from the system, thereby making it less productive, as the Pd^{2+} was removed, over time. In the case of glassy carbon under alternating polarity conditions, the reaction productivity initially increased and plateaued at a reaction time >2 hours. Competing reactions yielding methyl formate and formaldehyde were observed but could be partially inhibited by the presence of CO_2. Further increasing the concentration of CO_2 in the solution could further reduce the levels of **MF**, whilst exploring electrode materials capable of suppressing unnecessary methanol oxidation/reduction whilst being stable enough to use under alternating polarity conditions could reduce both **FA** and **MF** levels. Collectively, these results highlight the potential of alternating polarity methodologies in enhancing the yields and productivities of redox-

neutral electrochemical CO_2 utilisation, paving the way for more sustainable and scalable reaction methodologies.

Experimental

Further details of the experimental procedures, product analysis and additional supporting data can be found in the SI. Error bars are included in figures where multiple measurements under identical conditions were feasible. All experiments using glassy carbon electrodes were performed in triplicate and reported as mean with error bars indication standard deviation.

Experimental set up

All electrochemical experiments were conducted using an ElectraSyn™ 2.0 (IKA, Wilmington, NC). A standard 10 mL vial was modified with 2 mm O.D. inlet (*ca.* 15 mm from the bottom of the vessel) which allowed a continuous feed of gaseous CO_2 using Tygon® tubing (Saint Gobain Tygon® S3TM E-3603 Non-DEHP 1/16″ ID × 1/8″ OD). A mass flow controller (MFLX32907-51, Masterflex, Vernon Hills, IL) was used to control CO_2 flow rate and was connected using the same Tygon tubing. The PTFE electrode holder was used as supplied but was not sealed with a septum to prevent over-pressurisation.

For each experiment, CO_2 flow was 1 mL min^{-1} (1 sccm). The reaction medium consisted of 10 mL of 0.1 M LiBr in methanol and 5 mg $PdBr_2$. Two micro stir bars were used to stir the solution at 1500 rpm. The relevant electrical conditions were controlled and monitored using ElectraSyn™ 2.0.

Faradaic efficiency and productivity calculations

Faradaic efficiencies were calculated for dimethyl carbonate (**DMC**), formaldehyde (**FA**), and methyl formate (**MF**) were calculated based on the total charge (Q) passed and the number of moles of product formed (n) by using the following equations, all expressed in %.

$$\mathrm{FE}\,(\mathbf{DMC}) = \frac{2 \times n\mathbf{DMC}\,(\mathrm{mol}) \times 96\,485\,(\mathrm{C\,mol^{-1}})}{Q\,(\mathrm{C})} \times 100\%$$

$$\mathrm{FE}\,(\mathbf{FA}) = \frac{2 \times n\mathrm{Formaldehyde}\,(\mathrm{mol}) \times 96\,485\,(\mathrm{C\,mol^{-1}})}{Q\,(\mathrm{C})} \times 100\%$$

$$\mathrm{FE}\,(\mathbf{MF}) = \frac{2 \times n\mathrm{Methyl\ formate}\,(\mathrm{mol}) \times 96\,485\,(\mathrm{C\,mol^{-1}})}{Q\,(\mathrm{C})} \times 100\%$$

$$\mathrm{Productivity}\ \ (\mu\mathrm{mol\,h^{-1}}) = \frac{\mathrm{yield}\,(\mu\mathrm{mol})}{\mathrm{reaction\ time}\,(\mathrm{h})}$$

Conflicts of interest

There are no conflicts to declare.

Data availability

The data supporting this article have been included as part of the supplementary information (SI). Supplementary information is available, containing additional experimental details, characterisation and calculations. See DOI: https://doi.org/10.1039/d5gc02358k.

Acknowledgements

This work was supported through the generous funding from the Heintzelman Carbon Sequestration Fund. MI is grateful for support from the Yale School of the Environment Doctoral Training Fellowship. DSL gratefully acknowledges support from Nottingham Trent University. The authors wish to acknowledge the colleagues at the Center for Green Chemistry & Green Engineering at Yale for their continued support and advice in this study. The authors also acknowledge the use of equipment in the Catalysis and Separations Core at Yale University and extend their gratitude to Drs Xiaofan Jia and Nicholas Smith. We sincerely thank Dr Min Li and the Materials Characterisation Core at Yale University West Campus for their support and guidance on characterisation. Thank you to Dr Zhenting Jiang and Dr Dan Asael, Department of Geology and Geophysics at Yale University, for their assistance with SEM-EDX and ICP-MS, respectively. Finally, we thank Daryl Smith and Preston Smith from the Yale Glass Shop for their assistance in modifying the glass vessels.

References

1 J. Huo, Z. Wang, C. Oberschelp, G. Guillén-Gosálbez and S. Hellweg, *Green Chem.*, 2023, **25**, 415–430.
2 S. C. Peter, *ACS Energy Lett.*, 2018, **3**, 1557–1561.
3 R. Muthuraj and T. Mekonnen, *Polymer*, 2018, **145**, 348–373.
4 A. Otto, T. Grube, S. Schiebahn and D. Stolten, *Energy Environ. Sci.*, 2015, **8**, 3283–3297.
5 H. O. LeClerc, H. C. Erythropel, A. Backhaus, D. S. Lee, D. R. Judd, M. M. Paulsen, M. Ishii, A. Long, L. Ratjen, G. Gonsalves Bertho, C. Deetman, Y. Du, M. K. M. Lane, P. V. Petrovic, A. T. Champlin, A. Bordet, N. Kaeffer, G. Kemper, J. B. Zimmerman, W. Leitner and P. T. Anastas, *ACS Sustainable Chem. Eng.*, 2025, **13**(1), 5–29.
6 T. Biswal, K. P. Shadangi, P. K. Sarangi and R. K. Srivastava, *Chemosphere*, 2022, **298**, 134299.
7 S. A. Al-Tamreh, M. H. Ibrahim, M. H. El-Naas, J. Vaes, D. Pant, A. Benamor and A. Amhamed, *ChemElectroChem*, 2021, **8**, 3207–3220.
8 E. Schuler, M. Morana, P. A. Ermolich, K. Lüschen, A. J. Greer, S. F. R. Taylor, C. Hardacre, N. R. Shiju and G.-J. M. Gruter, *Green Chem.*, 2022, **24**, 8227–8258.
9 C. Chen, M. Garedew and S. W. Sheehan, *ACS Energy Lett.*, 2022, **7**, 988–992.

10 G. Trapasso, F. Russo, F. Galiano, C. R. McElroy, J. Sherwood, A. Figoli and F. Aricò, *ACS Sustainable Chem. Eng.*, 2023, **11**, 3390–3404.
11 P. Tundo, M. Musolino and F. Aricò, *Front. Chem.*, 2019, **7**, 300.
12 S.-H. Pyo, J. H. Park, T.-S. Chang and R. Hatti-Kaul, *Curr. Opin. Green Sustainable Chem.*, 2017, **5**, 61–66.
13 G. Fiorani, A. Perosa and M. Selva, *Green Chem.*, 2018, **20**, 288–322.
14 G. Yang, Q. Wang, L. Li, D. Lyu, H. Lin and D. Han, *Fuel*, 2025, **386**, 134221.
15 A. O. Esan, A. D. Adeyemi and S. Ganesan, *J. Cleaner Prod.*, 2020, **257**, 120561.
16 V. Farkas, M. Nagyházi, P. T. Anastas, J. Klankermayer and R. Tuba, *ChemSusChem*, 2023, **16**, e202300553.
17 H. Suo, H. Tang, R. Qu, J. Liu and Y. Qin, in *Advances in Bioenergy*, ed. Y. Li, Elsevier, 2024, vol. 9, pp. 171–246.
18 S. Ye, S. Wang, L. Lin, M. Xiao and Y. Meng, *Adv. Ind. Eng. Polym. Res.*, 2019, **2**, 143–160.
19 P. Tundo and M. Selva, *Acc. Chem. Res.*, 2002, **35**, 706–716.
20 M. A. Pacheco and C. L. Marshall, *Energy Fuels*, 1997, **11**, 2–29.
21 P. Tundo and F. Aricò, *ChemSusChem*, 2023, **16**, e202300748.
22 J. D. Medrano-García, J. Javaloyes-Antón, D. Vázquez, R. Ruiz-Femenia and J. A. Caballero, *J. CO2 Util.*, 2021, **45**, 101436.
23 H. Ohno, M. Ikhlayel, M. Tamura, K. Nakao, K. Suzuki, K. Morita, Y. Kato, K. Tomishige and Y. Fukushima, *Green Chem.*, 2021, **23**, 457–469.
24 S. Kim, S. G. Lee and D. H. Jeong, *Chem. Eng. Res. Des.*, 2024, **203**, 630–639.
25 V. Kontou, D. Grimekis, K. Braimakis and S. Karellas, *Renewable Sustainable Energy Rev.*, 2022, **157**, 112006.
26 M. F. O'Neill, M. Sankar and U. Hintermair, *ACS Sustainable Chem. Eng.*, 2022, **10**, 5243–5257.
27 G. M. Martins, G. C. Zimmer, S. R. Mendes and N. Ahmed, *Green Chem.*, 2020, **22**, 4849–4870.
28 B. A. Frontana-Uribe, R. D. Little, J. G. Ibanez, A. Palma and R. Vasquez-Medrano, *Green Chem.*, 2010, **12**, 2099–2119.
29 J. Rodríguez-Varela, I. L. Alonso-Lemus, O. Savadogo and K. Palaniswamy, *J. Mater. Res.*, 2021, **36**, 4071–4083.
30 Y. H. Budnikova, E. L. Dolengovski, M. V. Tarasov and T. V. Gryaznova, *J. Solid State Electrochem.*, 2024, **28**, 659–676.
31 J. R. Vanhoof, S. Spittaels and D. E. De Vos, *EES Catal.*, 2024, **2**, 753–779.
32 Y.-Y. Xie and Y.-M. Pan, *Green Chem.*, 2024, **26**, 9599–9618.
33 D. Anastasiadou, E. J. M. Hensen and M. C. Figueiredo, *Chem. Commun.*, 2020, **56**, 13082–13092.
34 C. Lu, S. Yang, P. Shi, S. Huang, C. Cai, J. Zhu, X. Zhuang and T. Wang, *Angew. Chem., Int. Ed.*, 2025, **64**, e202502846.
35 S. Choi, M. Balamurugan, K.-G. Lee, K. H. Cho, S. Park, H. Seo and K. T. Nam, *J. Phys. Chem. Lett.*, 2020, **11**, 2941–2948.
36 K. M. Lee, J. H. Jang, M. Balamurugan, J. E. Kim, Y. I. Jo and K. T. Nam, *Nat. Energy*, 2021, **6**(7), 733–741.
37 X. Li, S. G. Han, W. Wu, K. Zhang, B. Chen, S. H. Zhou, D. D. Ma, W. Wei, X. T. Wu, R. Zou and Q. L. Zhu, *Energy Environ. Sci.*, 2023, **16**, 502–512.
38 K. A. Wang, Z. L. Wang, H. C. Hu, H. Zhu and H. Yang, *Chem. Eng. J.*, 2024, **498**, 155109.
39 S.-G. Han, S. Zhou, X. Li, J. Zhao, W.-B. Wei, L. Zheng, D.-D. Ma, X.-T. Wu and Q.-L. Zhu, *Chem. Eng. J.*, 2024, **486**, 150179.
40 N. Fujinuma, N. Page, A. G. Boddy, J. Rivkind, L. Tomlinson, E. P. Hoy and S. E. Lofland, *Adv. Funct. Mater.*, 2025, **35**, 2412402.
41 G. Leonzio, A. Hankin and N. Shah, *Chem. Eng. Res. Des.*, 2024, **208**, 934–955.
42 C. Jia, Q. Sun and C. Zhao, *Chem. Commun.*, 2023, **59**, 7731–7742.
43 M. Šarić, B. J. V. Davies, N. C. Schjødt, S. Dahl, P. G. Moses, M. Escudero-Escribano, M. Arenz and J. Rossmeisl, *Green Chem.*, 2019, **21**, 6200–6209.
44 Y. Kawamata, K. Hayashi, E. Carlson, S. Shaji, D. Waldmann, B. J. Simmons, J. T. Edwards, C. W. Zapf, M. Saito and P. S. Baran, *J. Am. Chem. Soc.*, 2021, **143**, 16580–16588.
45 C. Schotten, C. J. Taylor, R. A. Bourne, T. W. Chamberlain, B. N. Nguyen, N. Kapur and C. E. Willans, *React. Chem. Eng.*, 2021, **6**, 147–151.
46 H. Li, J. Peng, L. Zeng, L. Zhou, M. Shabbir, F. Xiao, J. Yuan, H. Yi and A. Lei, *Green Chem.*, 2024, **26**, 11177–11181.
47 Y. Kawamata and P. S. Baran, *J. Synth. Org. Chem., Jpn.*, 2023, **81**(11), 1020–1027.
48 C. A. Obasanjo, G. Gao, B. N. Khiarak, T. H. Pham, J. Crane and C.-T. Dinh, *Energy Fuels*, 2023, **37**, 13601–13623.
49 Y. Xu, J. P. Edwards, S. Liu, R. K. Miao, J. E. Huang, C. M. Gabardo, C. P. O'Brien, J. Li, E. H. Sargent and D. Sinton, *ACS Energy Lett.*, 2021, **6**, 809–815.
50 R. Casebolt, K. Levine, J. Suntivich and T. Hanrath, *Joule*, 2021, **5**, 1987–2026.
51 J. Pertuiset, M. Gibilaro, O. Lemoine, P. Chamelot, G. Bourges and L. Massot, *Electrochim. Acta*, 2023, **439**, 141598.
52 A. J. Bard and L. R. Faulkner, *Electrochemical Methods: Fundamentals and Applications*, Wiley, 2012.
53 F. Schwarz, E. Larenz and A. K. Mechler, *Green Chem.*, 2024, **26**, 4645–4652.
54 K. A. Wang, Z. L. Wang and H. Zhu, *ChemSusChem*, 2024, **17**(9), e202301691.
55 A. Goyal, G. Marcandalli, V. A. Mints and M. T. M. Koper, *J. Am. Chem. Soc.*, 2020, **142**, 4154–4161.